

Supporting Information

Regulating luminescent thermal enhancement in negative thermal expansion metal-organic frameworks

Liang Chen,^a Yili Cao,^{*a} Rui Ma,^a Hongmei Cao,^a Xin Chen,^a Kun Lin,^a Qiang Li,^a
Jinxia Deng,^a Chunyu Liu,^b Yilin Wang,^c Ling Huang^{*c} and Xianran Xing^{*a}

^aBeijing Advanced Innovation Center for Materials Genome Engineering, Institute of Solid State Chemistry, University of Science and Technology Beijing, Beijing, 100083, China.

^bDepartment of Chemistry, Key Laboratory of Organic Optoelectronics and Molecular Engineering of the Ministry of Education, Tsinghua University, Beijing 100084, P.R. China.

^cInstitute of Advanced Materials, Nanjing Tech University, Nanjing, 211816, China.

*Correspondence: yilicao@ustb.edu.cn; iamlhuang@njtech.edu.cn; xing@ustb.edu.cn;

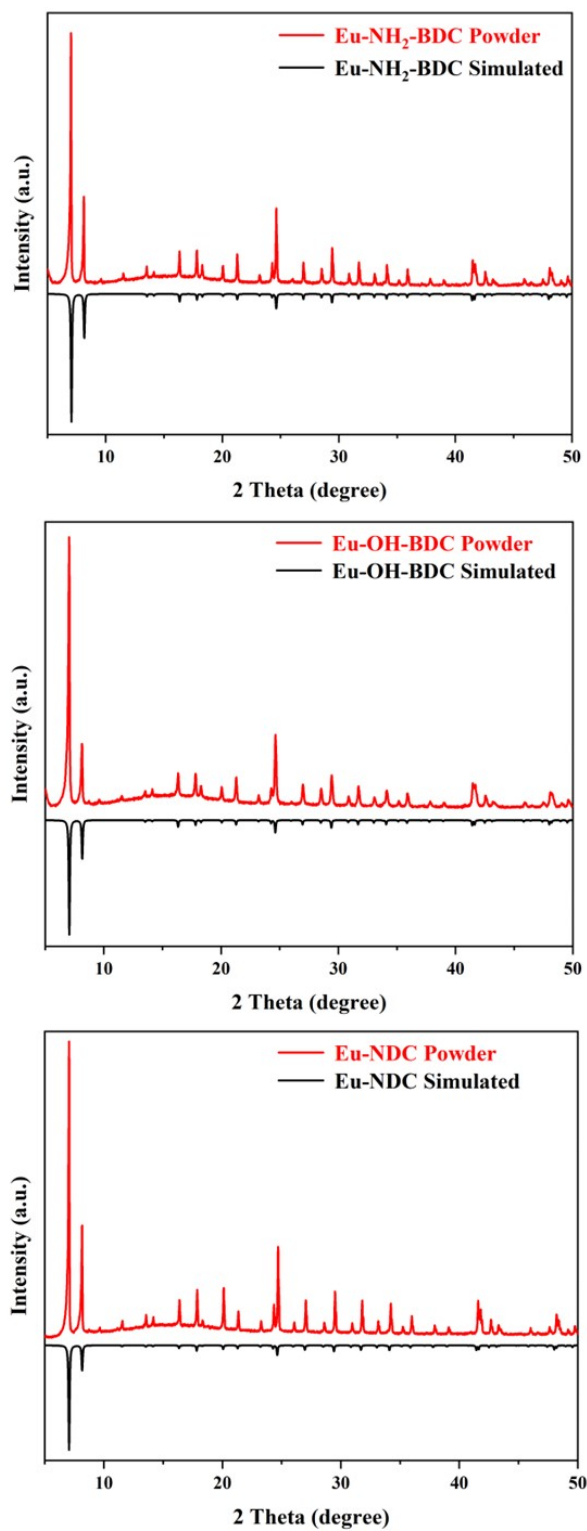


Figure S1. Powder X-Ray diffraction patterns of the activated powder of Eu-NH₂-BDC, Eu-OH-BDC, and Eu-NDC. The experimental patterns are compared to the simulated pattern based on the refined activated single crystal structures. Powder patterns were simulated from SCXRD structures using Mercury.¹

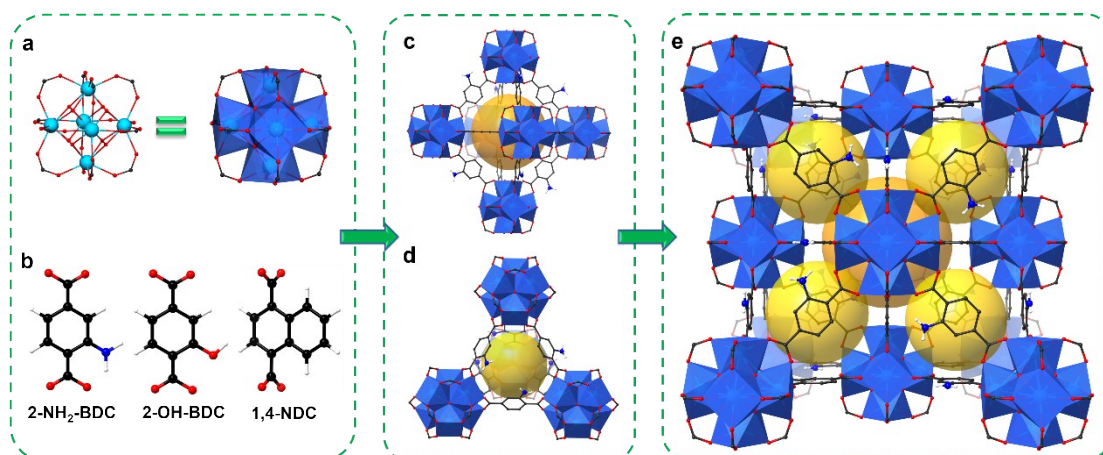


Figure S2. Schematic illustration of the structure of Eu-based isomeric MOFs with Eu-NH₂-BDC as an example. All hydrogens are omitted except for the hydrogen on the amino group for clarity. (Color code: Eu, sky blue; O, red; N, blue; C, black; H, white). (a) The 12-connected molecular building block. (b) The ligands with different functional groups. (c) The tetrahedral cage (green sphere) constructed from 6 molecular building blocks and 12 ligands. (d) The octahedral cage (yellow sphere) constructed from 4 molecular building blocks and 6 ligands. (e) The 3D network structure of Eu-NH₂-BDC.

Optical Measurement

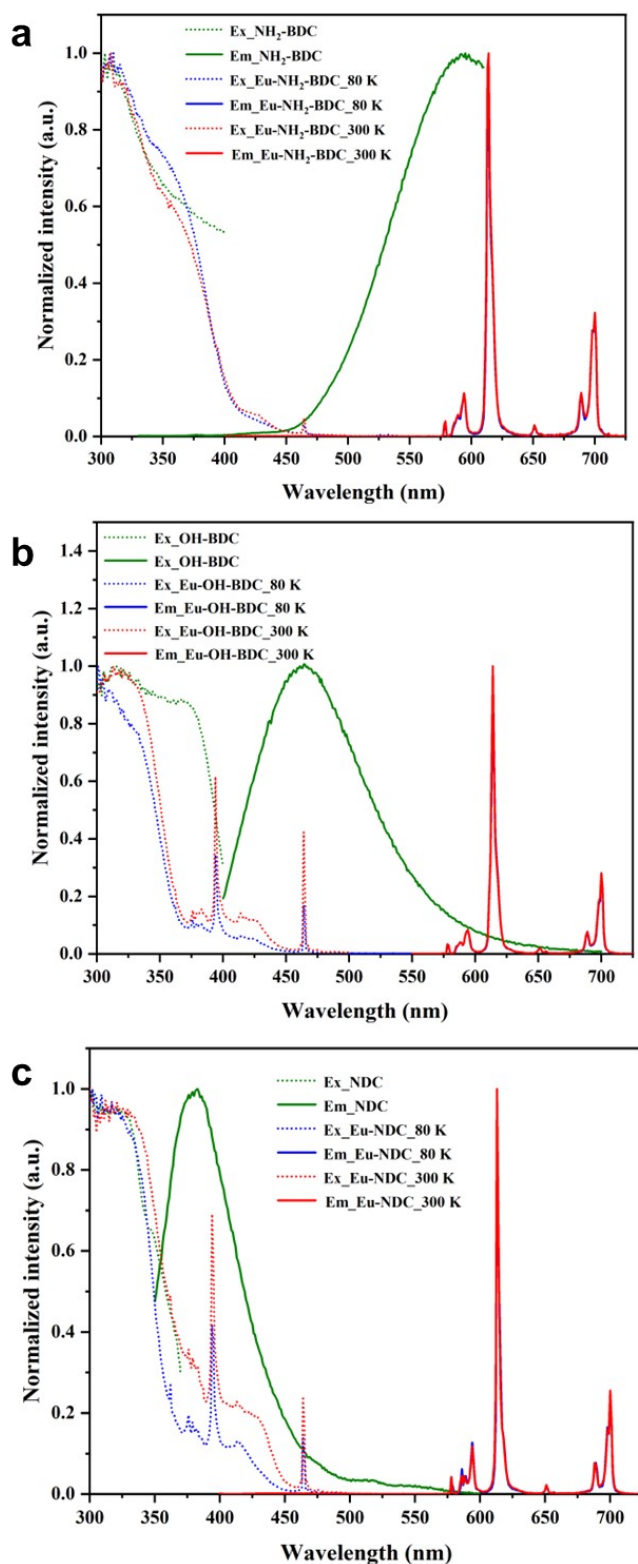


Figure S3. Photoluminescence excitation (dotted lines) and emission (solid lines) spectrum of (a) Eu-NH₂-BDC, (b) Eu-OH-BDC, and (c) Eu-NDC. The excitation and emission of the corresponding ligand for each structure are also included.

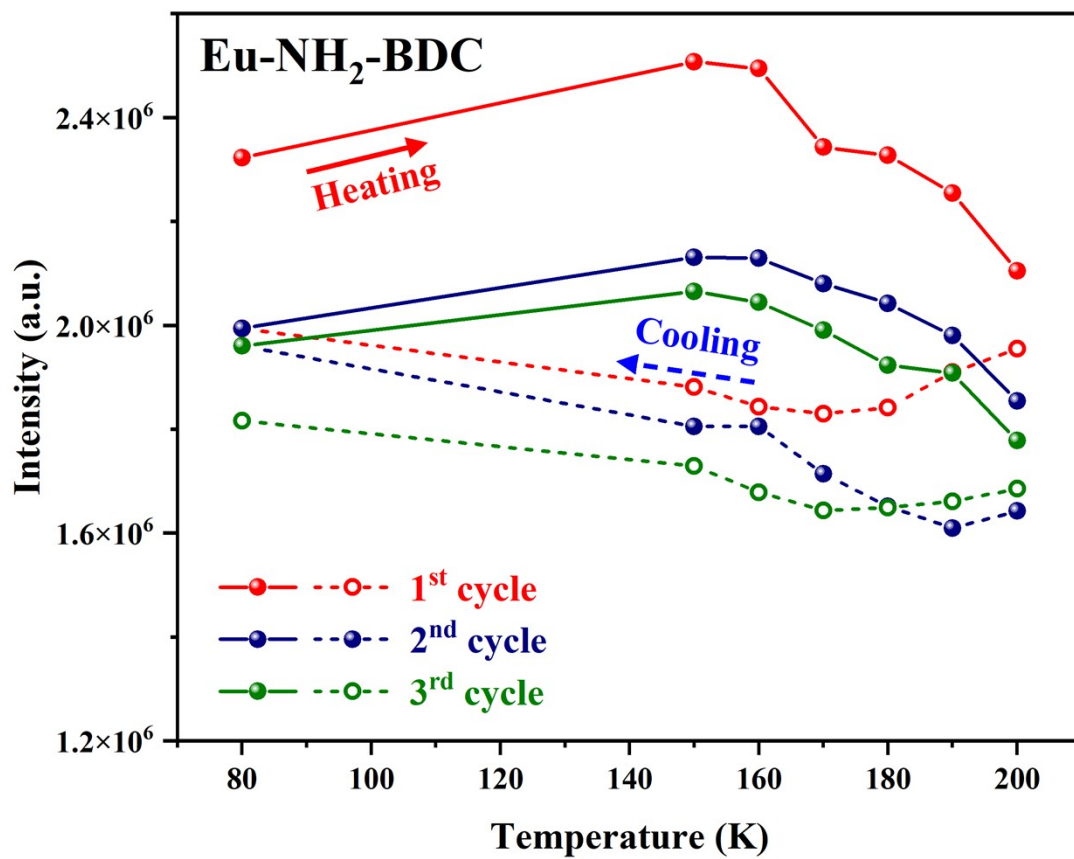


Figure S4. Reversibility of temperature-dependence of the maximum emission intensity of Eu-NH₂-BDC.

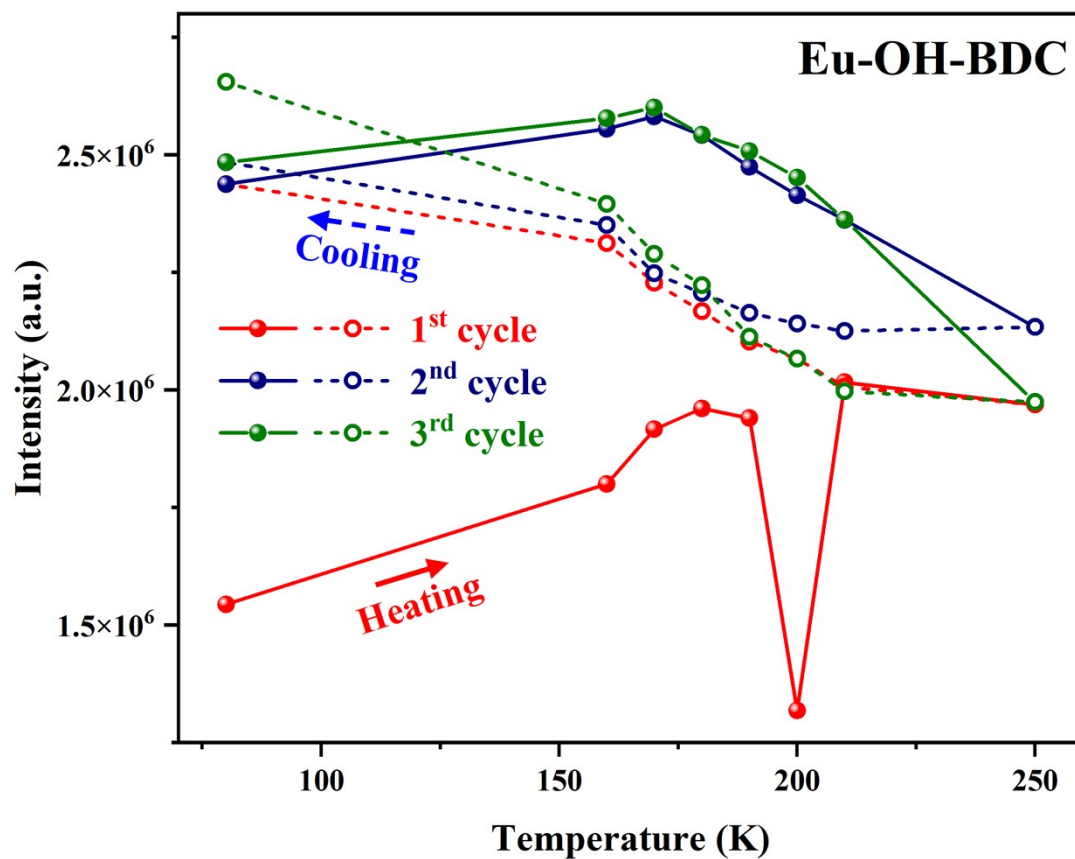


Figure S5. Reversibility of temperature-dependence of the maximum emission intensity of Eu-OH-BDC.

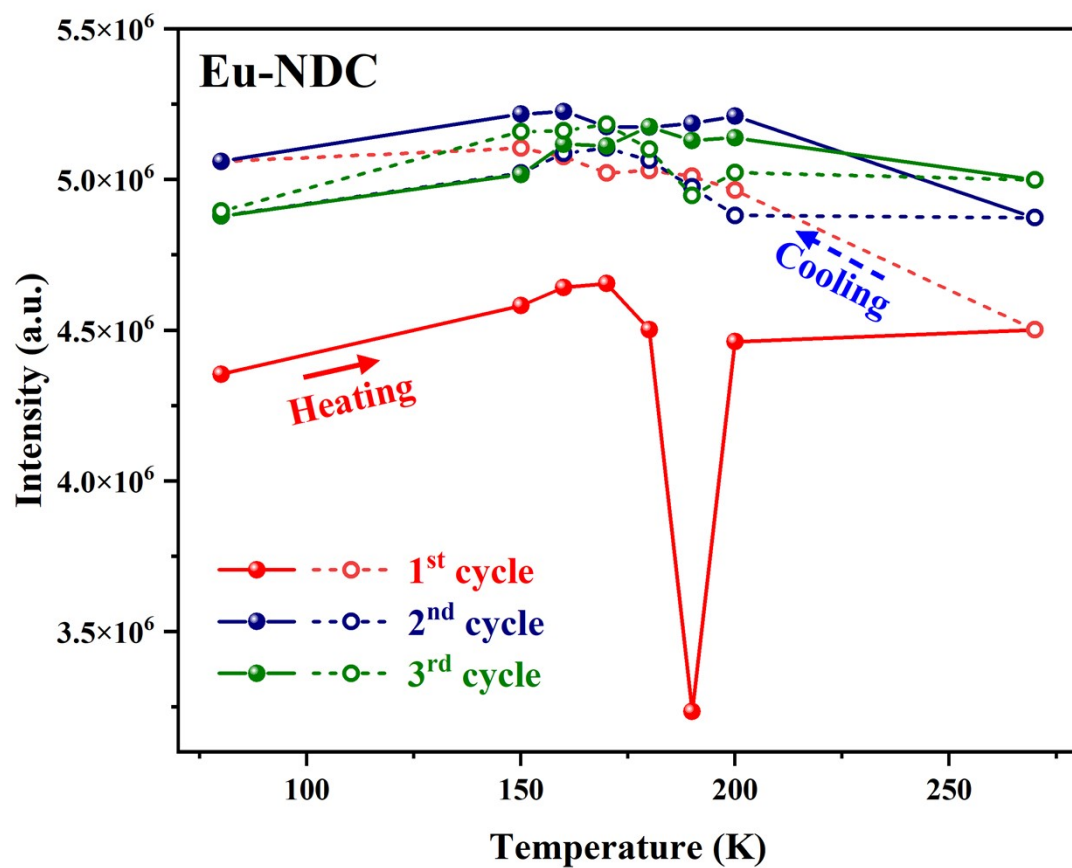


Figure S6. Reversibility of temperature-dependence of the maximum emission intensity of Eu-NDC.

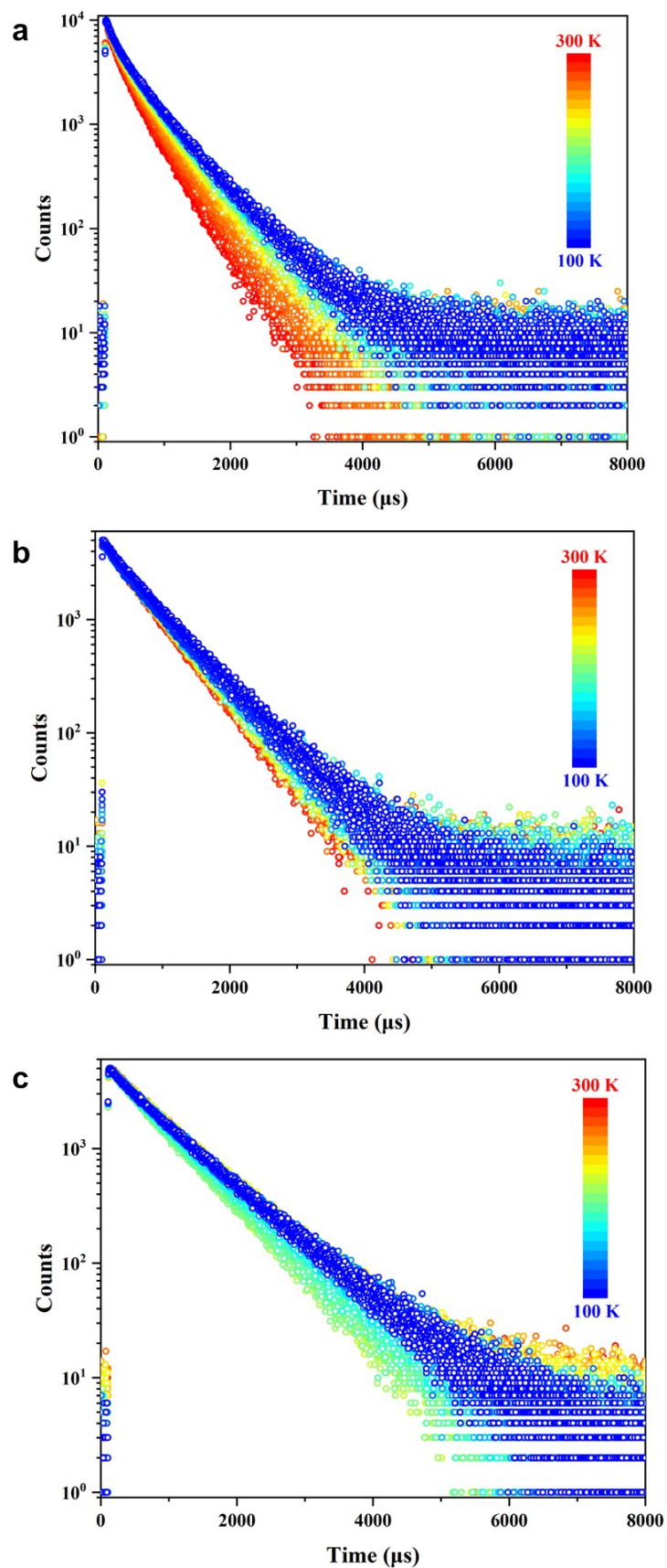


Figure S7. Decay curves as a function of temperature in (a) Eu-NH₂-BDC, (b) Eu-OH-BDC, and (c) Eu-NDC, respectively.

Table S1 Summary of photophysical properties for Eu-NH₂-BDC, Eu-OH-BDC and Eu-NDC at 300 K.

	λ_{ex} [nm]	Φ [%]	τ_{av} [μs]
Eu-NH ₂ -BDC	360	0.35	334.3
Eu-OH-BDC	394	1.92	561.0
Eu-NDC	394	5.67	740.4

λ_{ex} represent the wavelength of excitation, Φ is the PLQY, τ_{av} is the PL lifetime.

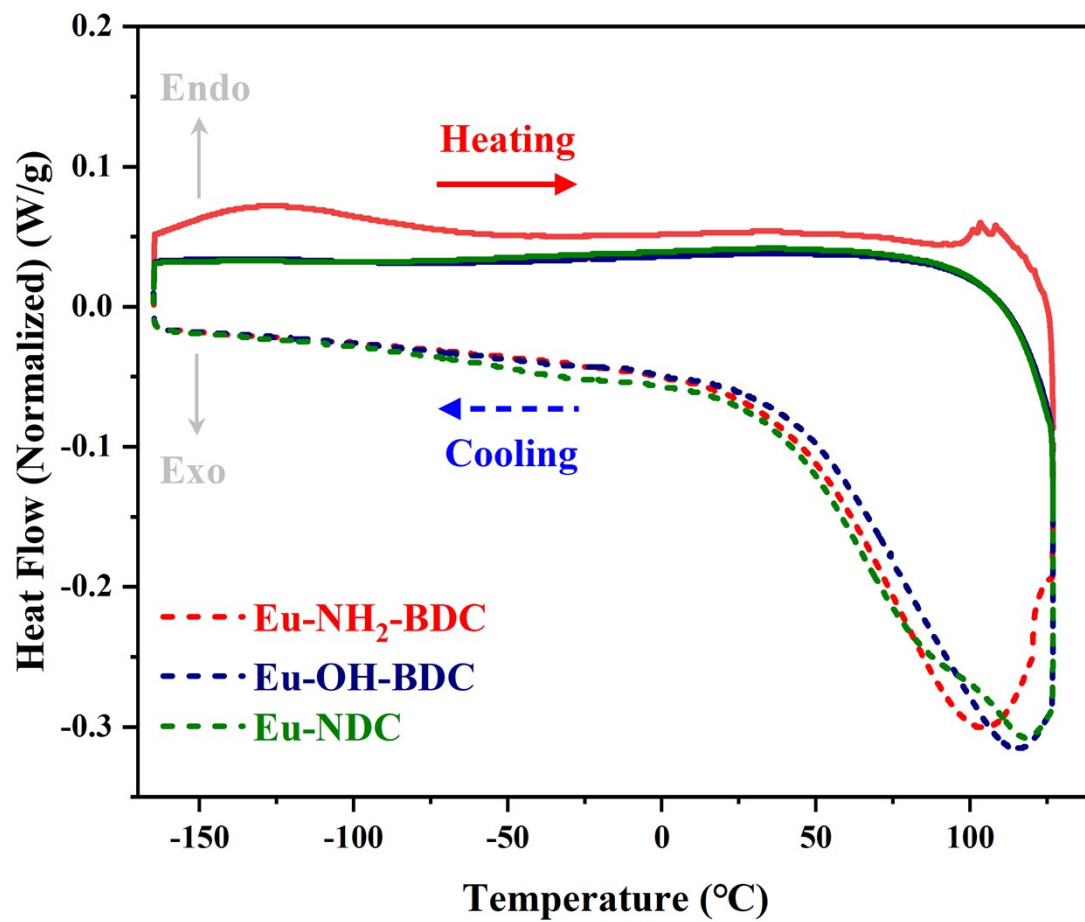


Figure S8. The DSC curves for Eu-NH₂-BDC, Eu-OH-BDC, and Eu-NDC under N₂ atmosphere (5 °C·min⁻¹).

First round of variable-temperature Powder X-ray diffraction (PXRD) data and Rietveld refinement

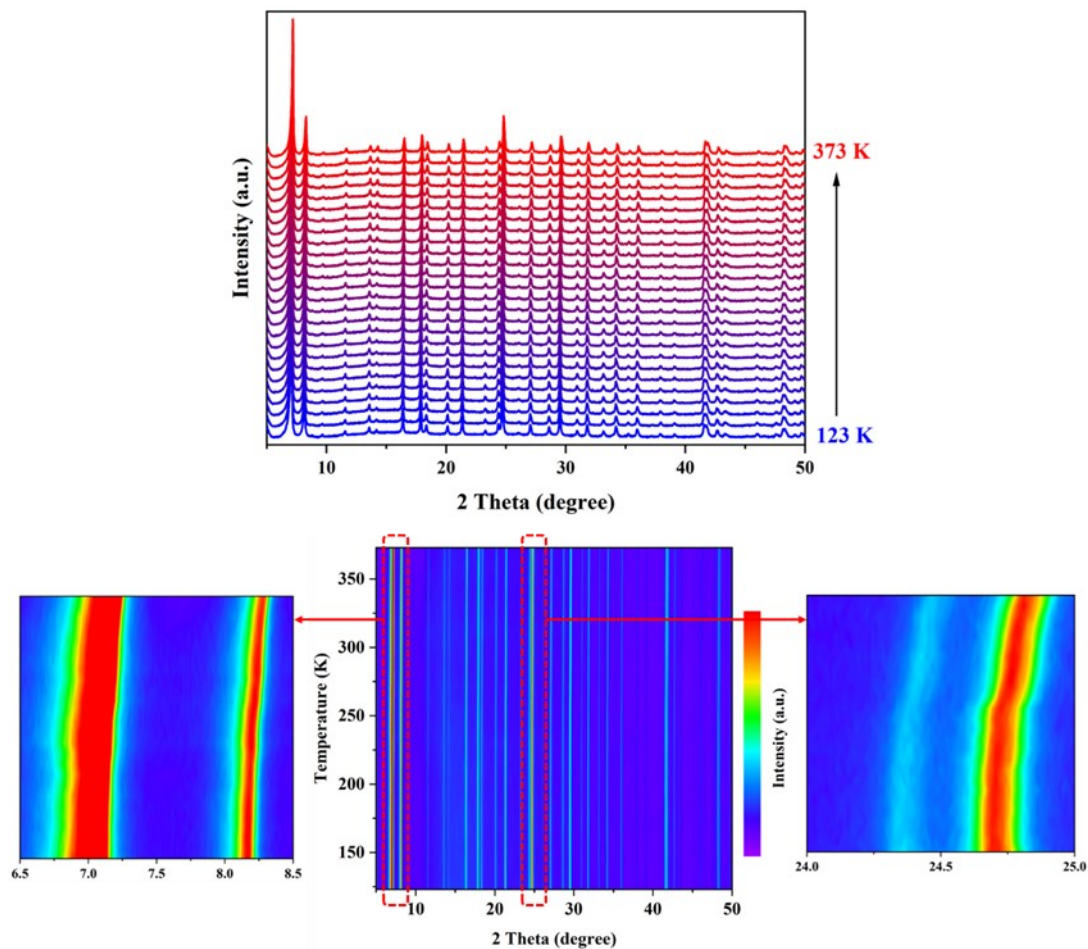


Figure S9. First round of variable-temperature PXRD patterns of Eu-NH₂-BDC (top) and 2D contours of Eu-NH₂-BDC (bottom).

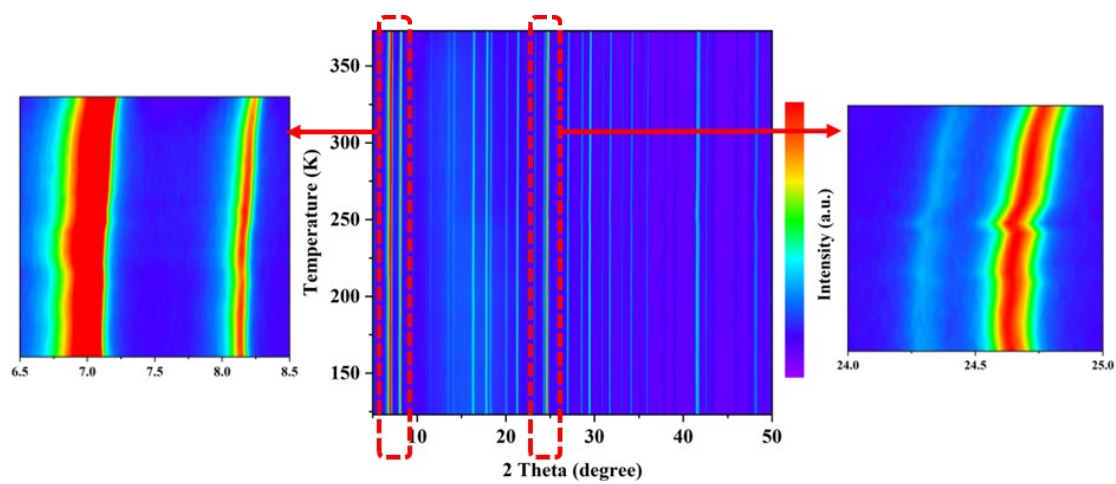
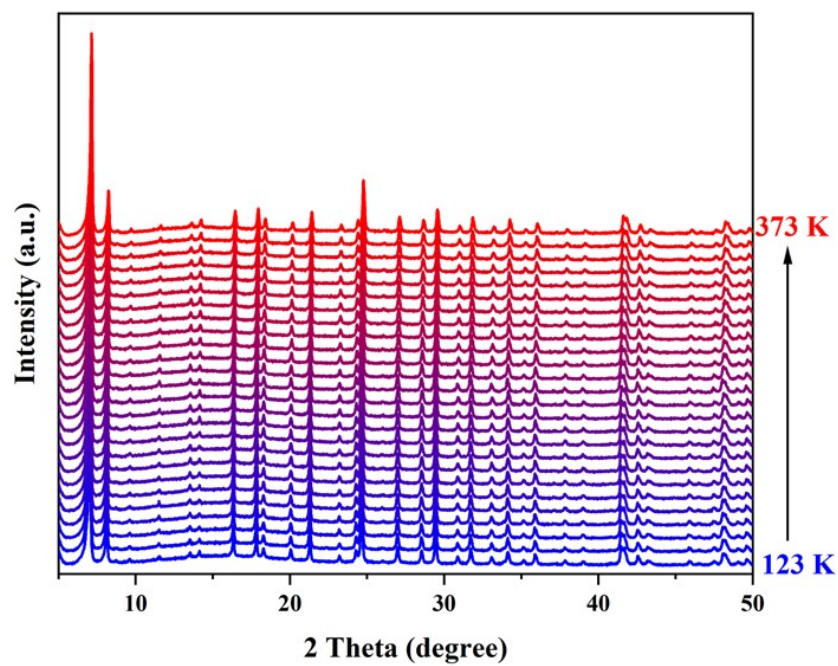


Figure S10. First round of variable-temperature PXRD patterns of Eu-OH-BDC (top) and 2D contours of Eu-OH-BDC (bottom).

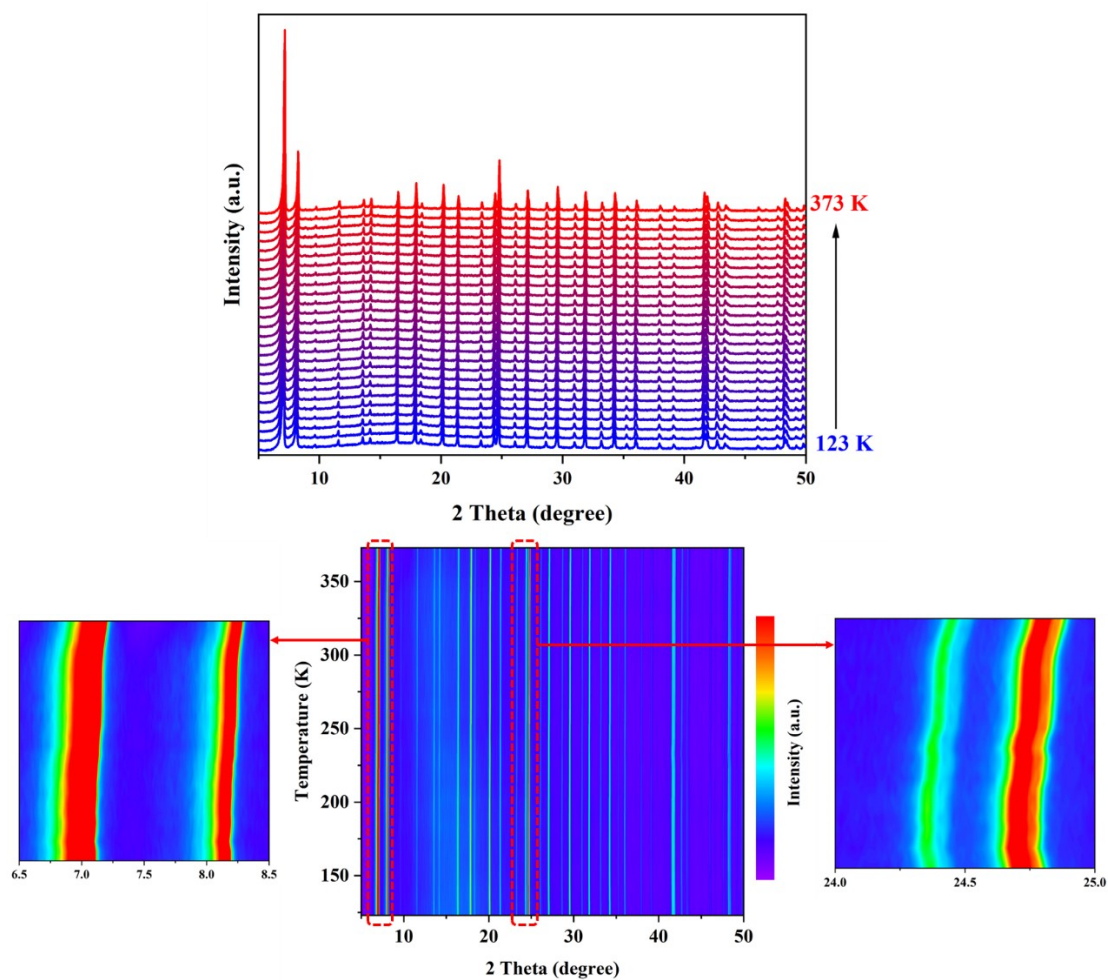


Figure S11. First round of variable-temperature PXRD patterns of Eu-NDC (top) and 2D contours of Eu-NDC (bottom).

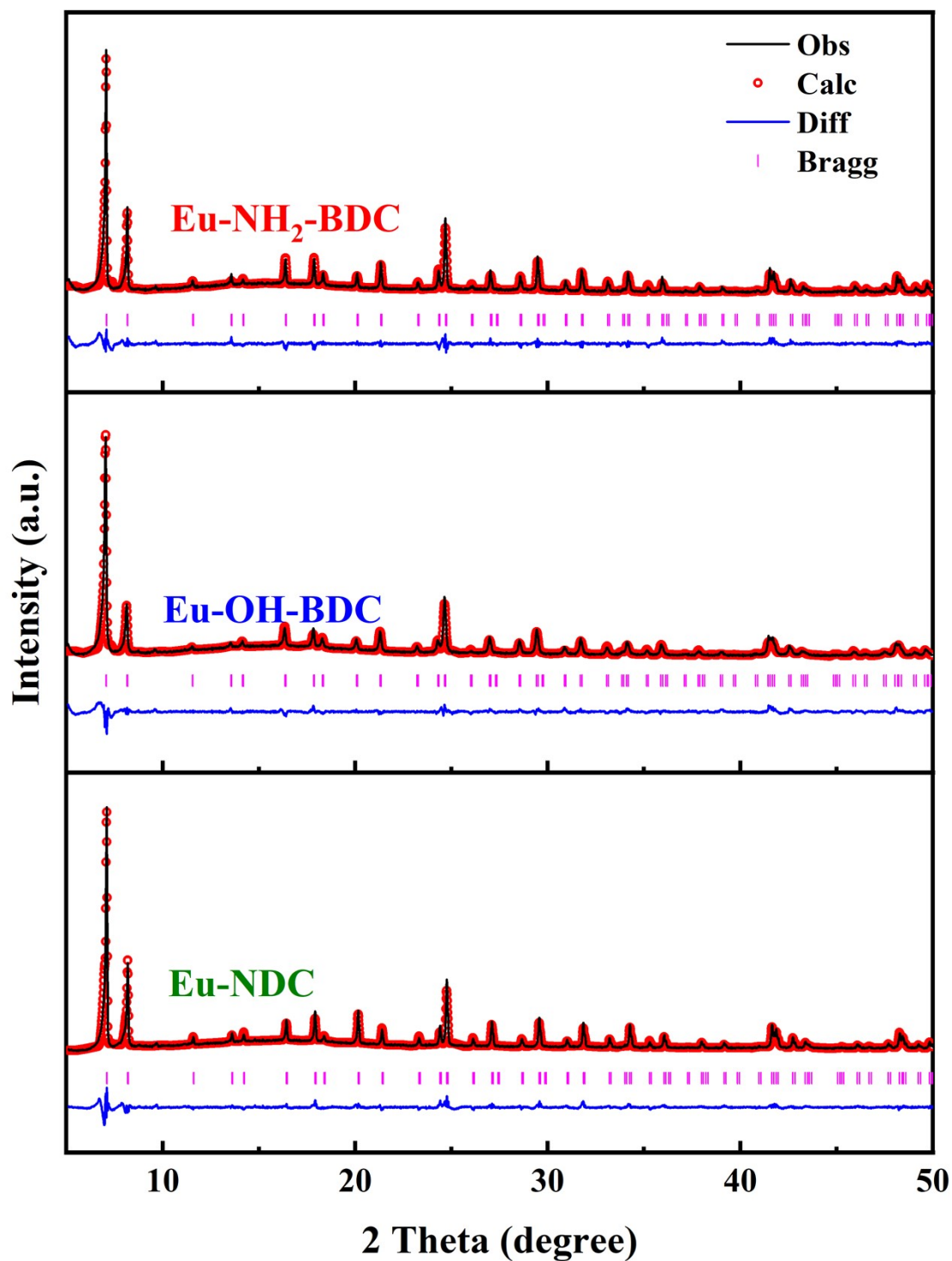


Figure S12. Rietveld refinement pattern of (a) Eu-NH₂-BDC, Eu-OH-BDC, and (c) Eu-NDC at 123 K, experiment data are given as black symbols, the fitted profile as red cycles, and the difference (data-fit) as blue line ($\chi^2 = 5.94$ for Eu-NH₂-BDC, $\chi^2 = 7.54$ for Eu-OH-BDC, $\chi^2 = 7.32$ for Eu-NDC)

Table S2 First round of variable-temperature lattice parameters of Eu-NH₂-BDC extracted from VTXRD using Rietveld refinement.

Temperature / K	$a / \text{\AA}$	$V / \text{\AA}^3$
123	21.61999	10105.70
133	21.62405	10111.40
143	21.62736	10116.04
153	21.62309	10110.05
163	21.62704	10115.59
173	21.62605	10114.20
183	21.62170	10108.10
193	21.62457	10112.13
203	21.62840	10117.50
213	21.62167	10108.06
223	21.61824	10103.25
233	21.61475	10098.36
243	21.60870	10089.88
253	21.61218	10094.75
263	21.60555	10085.47
273	21.60107	10079.19
283	21.59831	10075.33
293	21.5873	10059.93
303	21.58108	10051.24
313	21.57676	10045.20
323	21.56894	10034.28
333	21.55645	10016.86
343	21.54486	10000.71
353	21.53498	9986.96
363	21.52524	9973.42
373	21.5165	9961.27

Table S3 First round of variable-temperature lattice parameters of Eu-OH-BDC extracted from VTXRD using Rietveld refinement.

Temperature / K	$a / \text{\AA}$	$V / \text{\AA}^3$
123	21.65895	10160.43
133	21.6634	10166.70
143	21.66651	10171.08
153	21.66748	10172.44
163	21.66568	10169.91
173	21.66307	10166.23
183	21.65922	10160.81
193	21.6563	10156.70
203	21.65028	10148.24
213	21.64679	10143.33
223	21.63941	10132.96
233	21.63176	10122.22
243	21.62311	10110.08
253	21.64227	10136.98
263	21.62178	10108.21
273	21.60243	10081.10
283	21.5951	10070.84
293	21.59023	10064.03
303	21.5829	10053.78
313	21.57889	10048.18
323	21.57467	10042.28
333	21.56994	10035.68
343	21.56395	10027.32
353	21.55531	10015.27
363	21.54551	10001.62
373	21.53633	9988.84

Table S4 First round of variable-temperature lattice parameters of Eu-NDC extracted from VTXRD using Rietveld refinement.

Temperature / K	$a / \text{\AA}$	$V / \text{\AA}^3$
123	21.56304	10026.05
133	21.57005	10035.83
143	21.57706	10045.62
153	21.58078	10050.82
163	21.5793	10048.75
173	21.58069	10050.69
183	21.57983	10049.49
193	21.57985	10049.52
203	21.57593	10044.04
213	21.56977	10035.44
223	21.56569	10029.75
233	21.56873	10033.99
243	21.57017	10036.00
253	21.56512	10028.95
263	21.55603	10016.28
273	21.55209	10010.79
283	21.54958	10007.29
293	21.54854	10005.84
303	21.54777	10004.77
313	21.54709	10003.82
323	21.54551	10001.62
333	21.54349	9998.81
343	21.53829	9991.57
353	21.52779	9976.96
363	21.51976	9965.80
373	21.51261	9955.87

Second round of variable-temperature PXRD data and Rietveld refinement

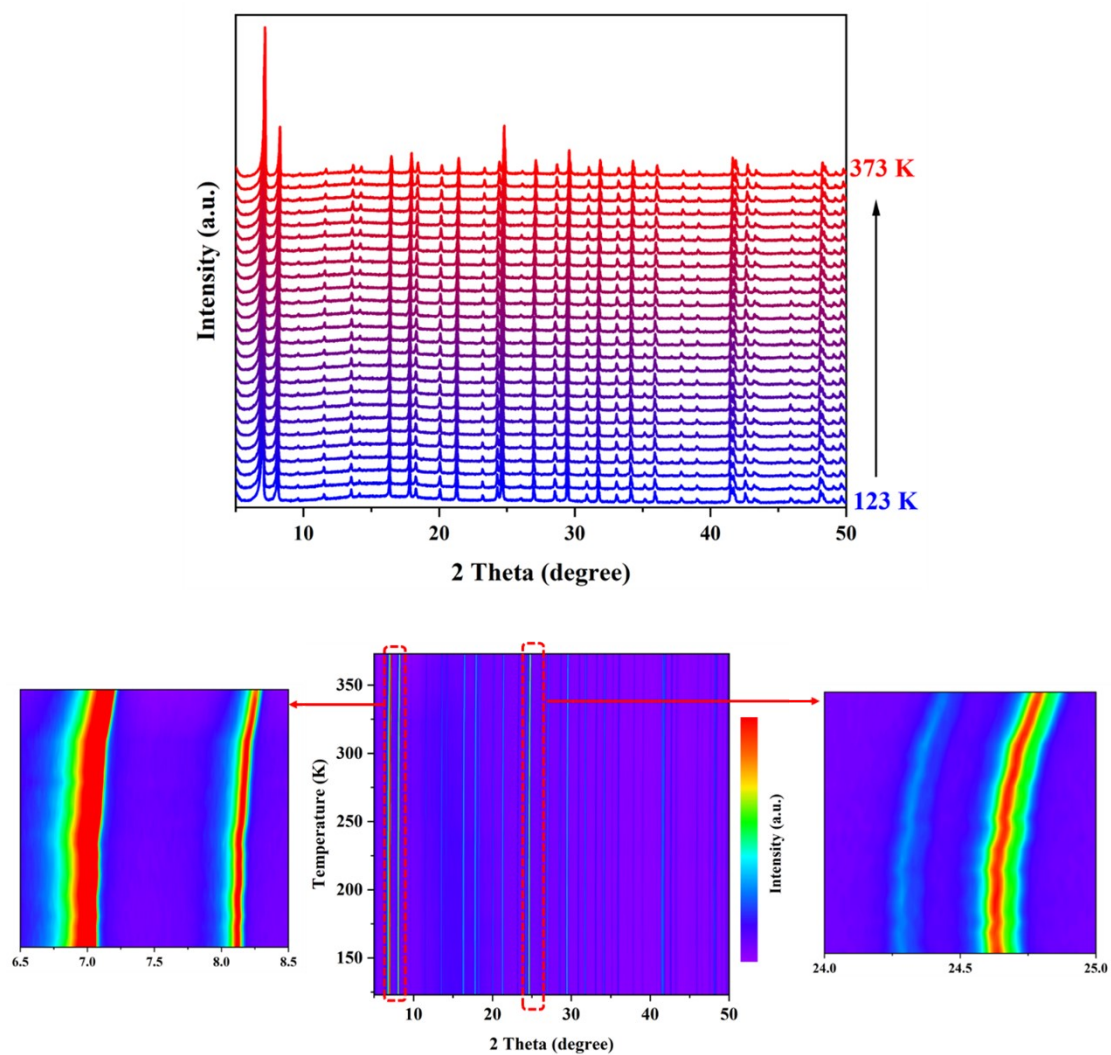


Figure S13. Second round of variable-temperature PXRD patterns of Eu-NH₂-BDC (top) and 2D contours of Eu-NH₂-BDC (bottom).

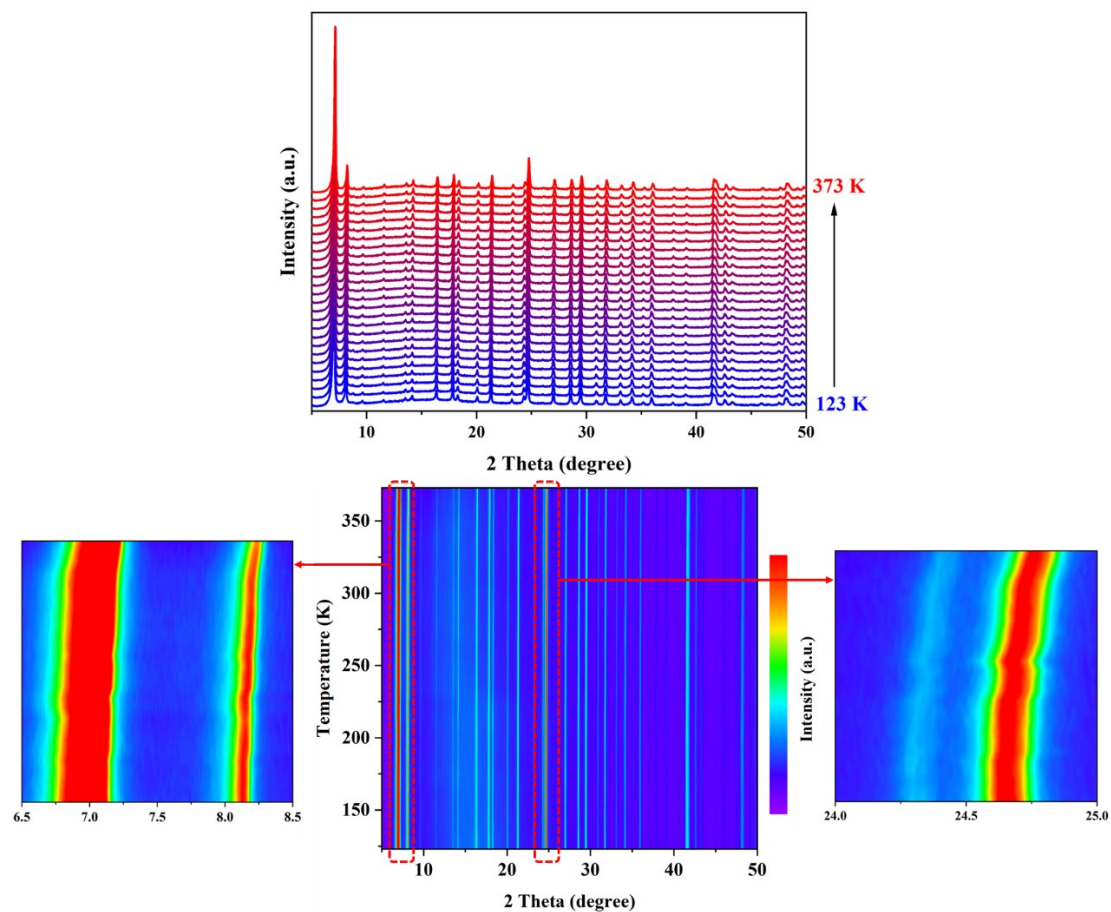


Figure S14. Second round of variable-temperature PXRD patterns of Eu-OH-BDC (top) and 2D contours of Eu-OH-BDC (bottom).

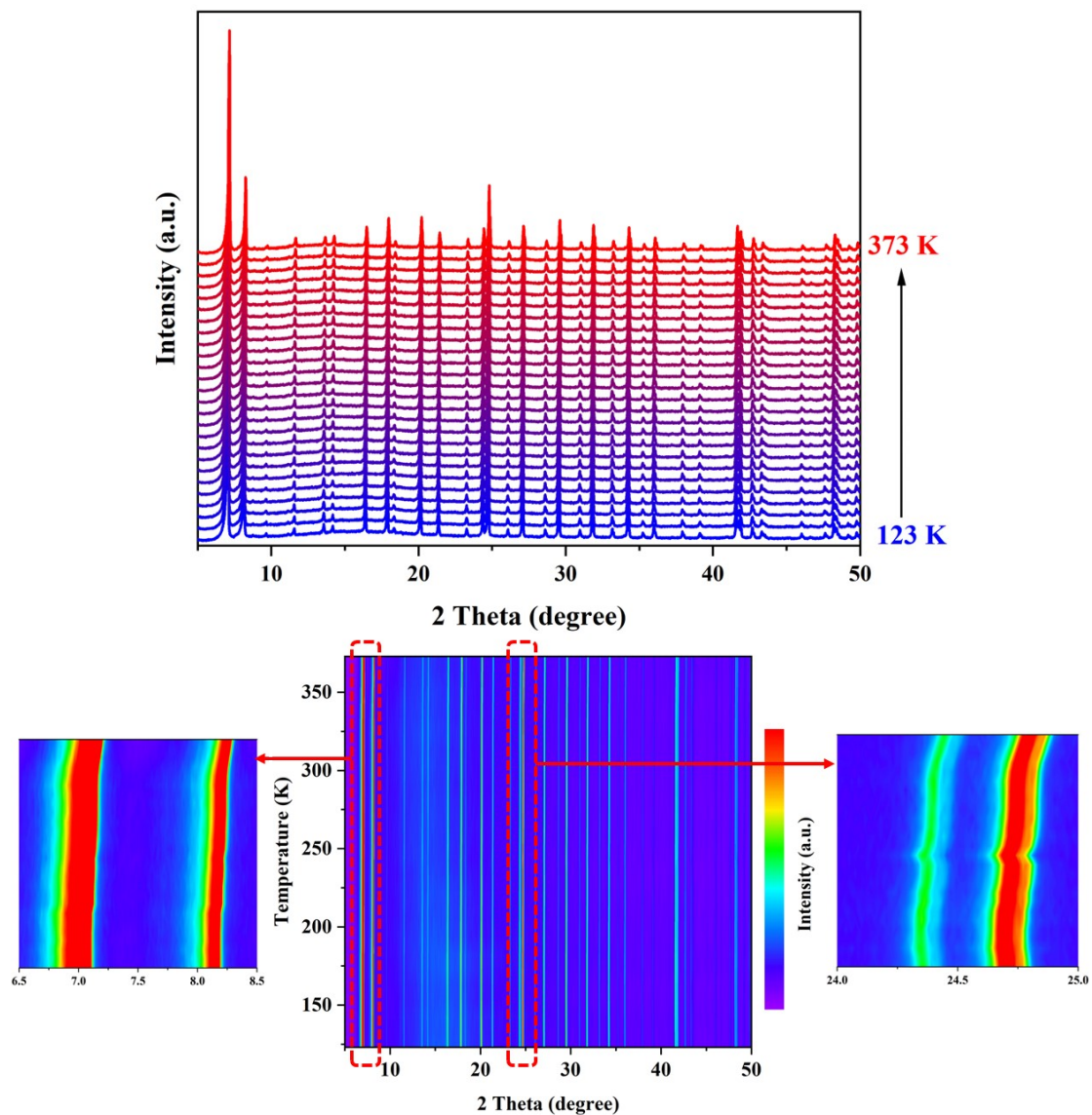


Figure S15. Second round of variable-temperature PXRD patterns of Eu-NDC (top) and 2D contours of Eu-NDC (bottom).

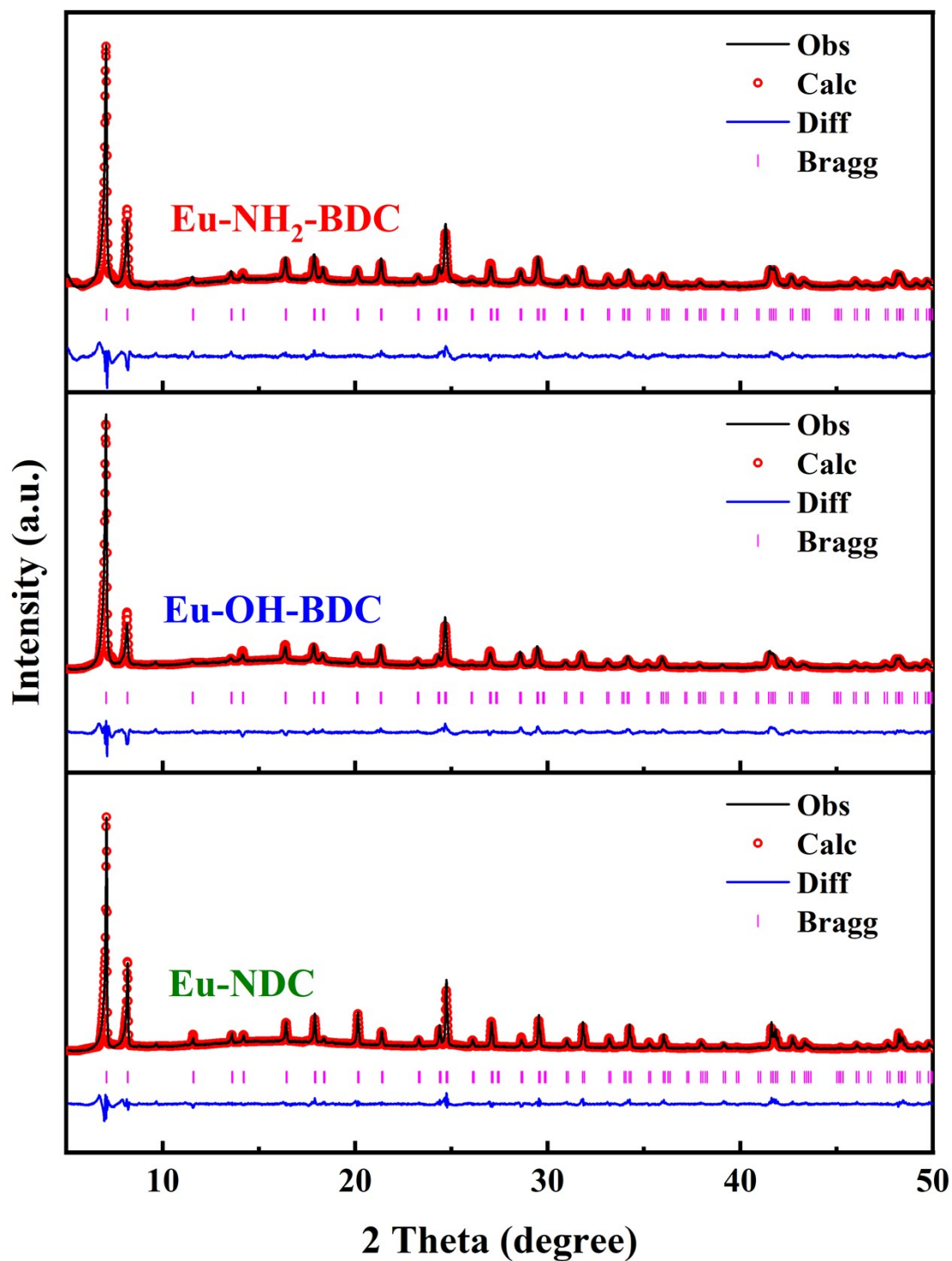


Figure S16. Rietveld refinement pattern of (a) Eu-NH₂-BDC, Eu-OH-BDC, and (c) Eu-NDC at 123 K, experiment data are given as black symbols, the fitted profile as red cycles, and the difference (data-fit) as blue line ($\chi^2 = 8.22$ for Eu-NH₂-BDC, $\chi^2 = 9.06$ for Eu-OH-BDC, $\chi^2 = 7.09$ for Eu-NDC).

Table S5 Second round of variable-temperature lattice parameters of Eu-NH₂-BDC extracted from VTXRD using Rietveld refinement.

Temperature / K	$a / \text{\AA}$	$V / \text{\AA}^3$
123	21.61994	10105.63
133	21.62223	10108.84
143	21.62207	10108.62
153	21.62205	10108.59
163	21.62046	10106.36
173	21.61961	10105.17
183	21.61783	10102.67
193	21.61967	10105.25
203	21.61843	10103.51
213	21.61386	10097.11
223	21.6107	10092.68
233	21.60859	10089.72
243	21.60621	10086.39
253	21.6067	10087.08
263	21.60234	10080.97
273	21.58834	10061.38
283	21.58079	10050.83
293	21.57429	10041.75
303	21.57152	10037.89
313	21.5678	10032.69
323	21.56447	10028.05
333	21.56068	10022.76
343	21.55594	10016.15
353	21.54996	10007.82
363	21.54261	9997.58
373	21.5342	9985.88

Table S6 Second round of variable-temperature lattice parameters of Eu-OH-BDC extracted from VTXRD using Rietveld refinement.

Temperature / K	$a / \text{\AA}$	$V / \text{\AA}^3$
123	21.63997	10133.74
133	21.64212	10136.77
143	21.64189	10136.44
153	21.64328	10138.40
163	21.6428	10137.72
173	21.63736	10130.08
183	21.63715	10129.78
193	21.63838	10131.51
203	21.63572	10127.78
213	21.63407	10125.46
223	21.63136	10121.65
233	21.62109	10107.24
243	21.61784	10102.69
253	21.61484	10098.48
263	21.62348	10110.60
273	21.61146	10093.74
283	21.60303	10081.94
293	21.59841	10075.47
303	21.59431	10069.73
313	21.5919	10066.36
323	21.58987	10063.52
333	21.58765	10060.42
343	21.58192	10052.41
353	21.57154	10037.91
363	21.56356	10026.78
373	21.55598	10016.21

Table S7 Second round of variable-temperature lattice parameters of Eu-NDC extracted from VTXRD using Rietveld refinement.

Temperature / K	$a / \text{\AA}$	$V / \text{\AA}^3$
123	21.57983	10049.49
133	21.58304	10053.98
143	21.58656	10058.90
153	21.58754	10060.27
163	21.58685	10059.30
173	21.58504	10056.77
183	21.58392	10055.21
193	21.58	10049.73
203	21.57837	10047.45
213	21.5716	10038.00
223	21.56856	10033.75
233	21.56702	10031.60
243	21.57923	10048.65
253	21.57315	10040.16
263	21.567	10031.58
273	21.56441	10027.96
283	21.5622	10024.88
293	21.56041	10022.38
303	21.56038	10022.34
313	21.55983	10021.58
323	21.55915	10020.63
333	21.55275	10011.71
343	21.54779	10004.80
353	21.53928	9992.95
363	21.52905	9978.71
373	21.5198	9965.86

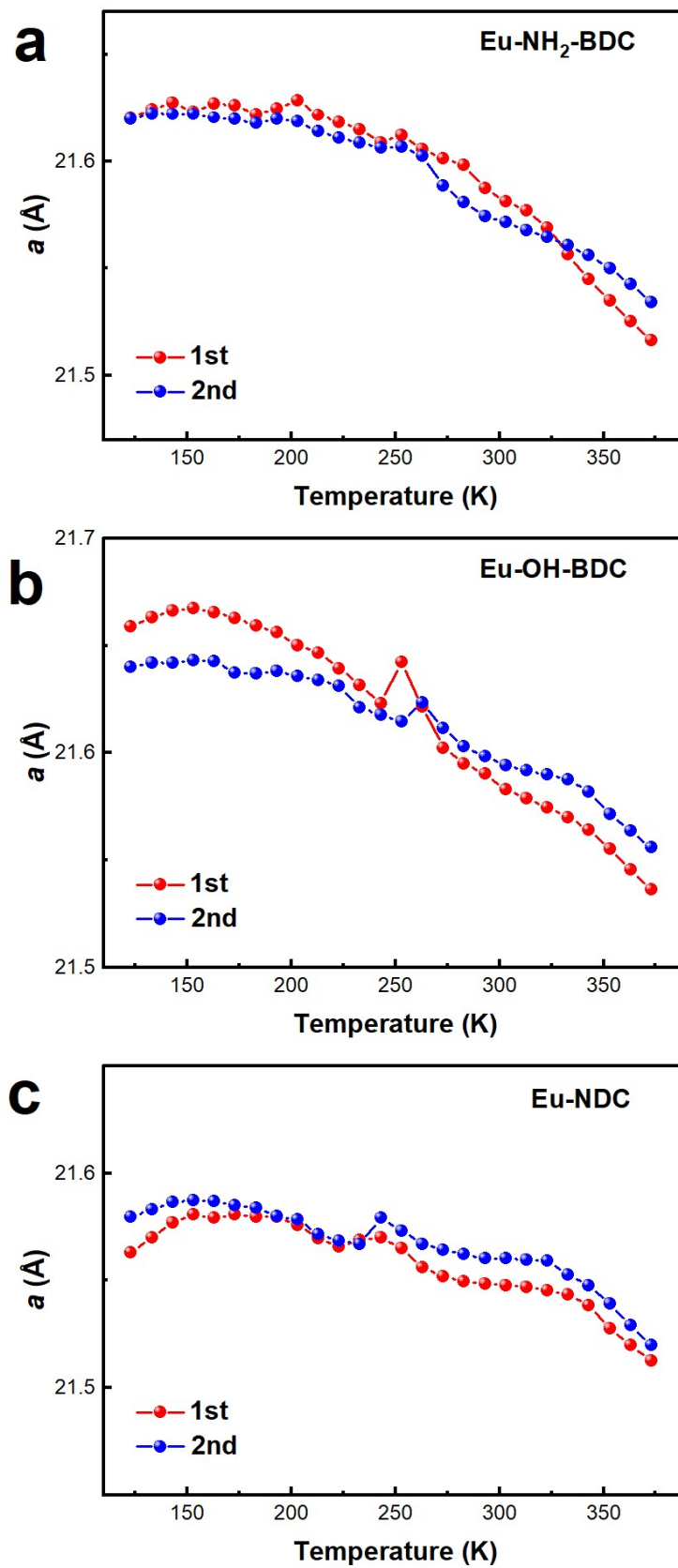


Figure S17. Comparison of two rounds of variable temperature PXRD trends for (a) Eu-NH₂-BDC, (b) Eu-OH-BDC, and (c) Eu-NDC.

Variable Temperature Single Crystal X-ray Diffraction (SCXRD) Analyses

Variable temperature single crystal X-ray diffraction measurements for activated Eu-MOFs were conducted at the X-ray crystallography platform of the Beijing Institute of Technology. The data were collected using a Rigaku XtaLAB Synergy Custom diffractometer with a Mo K α radiation ($\lambda = 0.71073 \text{ \AA}$) at 100, 150, 200, 250, and 300 K. The selected crystals were covered with paratone oil, and mounted onto the goniometer under the cold N₂ gas stream. Temperature control using the instrument software. The structures were solved by intrinsic phasing (SHELXT)² and refined by full-matrix least squares on F² (SHELXL-2019)³ on Olex2 software (ver. 1.5)⁴. All non-hydrogen atoms were refined anisotropically. The thermal constraint (ISOR, RIGU) was used for the structural refinement of the ligands.

Crystallographic data are summarized in Supplementary Table 8-10. Crystallographic information files (CIF) have been deposited in the Cambridge Crystallographic Data Centre (CCDC) under deposition number CCDC 2246487-2246501. The data can be obtained free of charge via www.ccdc.cam.ac.uk/data_request/cif (or from the Cambridge Crystallographic Data Centre, 12 Union Road, Cambridge CB2 1EZ, U.K.).

Table S8 Temperature-dependent crystallographic data of compound Eu-NH₂-BDC.

Eu-NH ₂ -BDC	100 K	150 K	200 K	250 K	300 K
Empirical formula	C ₉₆ Eu ₁₂ N ₁₂ O 64	C ₉₆ Eu ₁₂ N ₁₂ O 64	C ₉₆ Eu ₁₂ N ₁₂ O 64	C ₉₆ Eu ₁₂ N ₁₂ O 64	C ₉₆ Eu ₁₂ N ₁₂ O 64
Crystal system	cubic	cubic	cubic	cubic	cubic
Space group	<i>Fm</i> -3 <i>m</i>	<i>Fm</i> -3 <i>m</i>	<i>Fm</i> -3 <i>m</i>	<i>Fm</i> -3 <i>m</i>	<i>Fm</i> -3 <i>m</i>
<i>a</i> /Å	21.6551(8)	21.7212(8)	21.7226(9)	21.6449(8)	21.5913(7)
<i>b</i> /Å	21.6551(8)	21.7212(8)	21.7226(9)	21.6449(8)	21.5913(7)
<i>c</i> /Å	21.6551(8)	21.7212(8)	21.7226(9)	21.6449(8)	21.5913(7)
α /°	90	90	90	90	90
β /°	90	90	90	90	90
γ /°	90	90	90	90	90
<i>V</i> /Å ³	10155.0(11)	10248.3(11)	10250.3(13)	10140.7(11)	10065.5(10)
ρ_{calc} mg/mm ³	1.363	1.351	1.351	1.365	1.375
<i>Z</i>	2	2	2	2	2
μ (Mo K α)/mm ⁻¹	3.707	3.673	3.672	3.712	3.740
<i>F</i> (000)	3856.0	3856.0	3856.0	3856.0	3856.0
<i>R</i> ₁ ^a [<i>I</i> > 2 σ (<i>I</i>)]	0.0425(525)	0.0490(492)	0.0513(435)	0.0437(515)	0.0482(459)
<i>wR</i> ₂ ^b	0.1182(687)	0.1350(642)	0.1442(609)	0.1218(679)	0.1389(604)
GOF ^c	1.026	1.048	1.020	1.037	1.063
Data completeness	99.4	99.0	94.1	99.2	96.3
CCDC	2246487	2246488	2246489	2246490	2246491

^a $R = \sum ||F_o| - |F_c|| / \sum |F_o|$. ^b $wR = \{\sum w(F_o^2 - F_c^2)^2 / \sum w(F_o^2)^2\}^{1/2}$. ^c $GOF = \{\sum w((F_o^2 - F_c^2)^2) / (n - p)\}^{1/2}$, where

n = number of reflections and *p* = total number of parameters refined.

Table S9 Temperature-dependent crystallographic data of compound Eu-OH-BDC.

Eu-OH-BDC	100 K	150 K	200 K	250 K	300 K
Empirical formula	C ₉₆ Eu ₁₂ O ₇₆	C ₉₆ Eu ₁₂ O ₇₆	C ₉₆ Eu ₁₂ O ₇₆	C ₉₆ Eu ₁₂ O ₇₆	C ₉₆ Eu ₁₂ O ₇₆
Crystal system	cubic	cubic	cubic	cubic	cubic
Space group	<i>Fm</i> -3 <i>m</i>	<i>Fm</i> -3 <i>m</i>	<i>Fm</i> -3 <i>m</i>	<i>Fm</i> -3 <i>m</i>	<i>Fm</i> -3 <i>m</i>
<i>a</i> /Å	21.6800(12)	21.7434(16)	21.6439(12)	21.6136(13)	21.556(2)
<i>b</i> /Å	21.6800(12)	21.7434(16)	21.6439(12)	21.6136(13)	21.556(2)
<i>c</i> /Å	21.6800(12)	21.7434(16)	21.6439(12)	21.6136(13)	21.556(2)
α /°	90	90	90	90	90
β /°	90	90	90	90	90
γ /°	90	90	90	90	90
<i>V</i> /Å ³	10190.1(16)	10280(2)	10139.3(17)	10096.8(18)	10017(3)
ρ_{calc} mg/mm ³	1.366	1.354	1.373	1.379	1.390
<i>Z</i>	2	2	2	2	2
μ (Mo K α)/mm ⁻¹	3.697	3.665	3.716	3.731	3.761
<i>F</i> (000)	3880.0	3880.0	3880.0	3880.0	3880.0
<i>R</i> ₁ ^a [<i>I</i> > 2 σ (<i>I</i>)]	0.0922(519)	0.0913(458)	0.0875(481)	0.0786(425)	0.0670(454)
<i>wR</i> ₂ ^b	0.2331(720)	0.2249(637)	0.2384(699)	0.2022(615)	0.1753(687)
GOF ^c	1.037	1.105	1.080	1.071	1.013
Data completeness	99	98.3	97.5	96.5	98.4
CCDC	2246492	2246493	2246494	2246495	2246496

^a $R = \sum ||F_o| - |F_c|| / \sum |F_o|$. ^b $wR = \{ \sum w(F_o^2 - F_c^2)^2 / \sum w(F_o^2)^2 \}^{1/2}$. ^c $GOF = \{ \sum w((F_o^2 - F_c^2)^2) / (n - p) \}^{1/2}$, where *n* = number of reflections and *p* = total number of parameters refined.

Table S10 Temperature-dependent crystallographic data of compound Eu-NDC.

Eu-NDC	100 K	150 K	200 K	250 K	300 K
Empirical formula	C132Eu12O64	C132Eu12O64	C132Eu12O64	C132Eu12O64	C132Eu12O64
Crystal system	cubic	cubic	cubic	cubic	cubic
Space group	<i>Fm</i> -3 <i>m</i>	<i>Fm</i> -3 <i>m</i>	<i>Fm</i> -3 <i>m</i>	<i>Fm</i> -3 <i>m</i>	<i>Fm</i> -3 <i>m</i>
<i>a</i> /Å	21.6408(6)	21.6573(6)	21.6554(6)	21.6478(5)	21.5900(6)
<i>b</i> /Å	21.6408(6)	21.6573(6)	21.6554(6)	21.6478(5)	21.5900(6)
<i>c</i> /Å	21.6408(6)	21.6573(6)	21.6554(6)	21.6478(5)	21.5900(6)
α /°	90	90	90	90	90
β /°	90	90	90	90	90
γ /°	90	90	90	90	90
<i>V</i> /Å ³	10134.9(8)	10158.1(8)	10155.4(8)	10144.8(7)	10063.7(8)
ρ_{calc} mg/mm ³	1.453	1.449	1.450	1.451	1.463
<i>Z</i>	2	2	2	2	2
μ (Mo K α)/mm ⁻¹	3.718	3.709	3.710	3.714	3.744
<i>F</i> (000)	4120.0	4120.0	4120.0	4120.0	4120.0
<i>R</i> ₁ ^a [<i>I</i> > 2 σ (<i>I</i>)]	0.0464(537)	0.0438(541)	0.0426(539)	0.0437(546)	0.0476(519)
<i>wR</i> ₂ ^b	0.1220(630)	0.1189(631)	0.1114(633)	0.1205(635)	0.1286(630)
GOF ^c	1.084	1.176	1.106	1.133	1.074
Data completeness	99.2	99.2	99.4	99.4	99.6
CCDC	2246497	2246498	2246499	2246500	2246501

^a $R = \sum ||F_o| - |F_c|| / \sum |F_o|$. ^b $wR = \{ \sum w(F_o^2 - F_c^2)^2 / \sum w(F_o^2)^2 \}^{1/2}$. ^c $GOF = \{ \sum w((F_o^2 - F_c^2)^2) / (n - p) \}^{1/2}$, where *n* = number of reflections and *p* = total number of parameters refined.

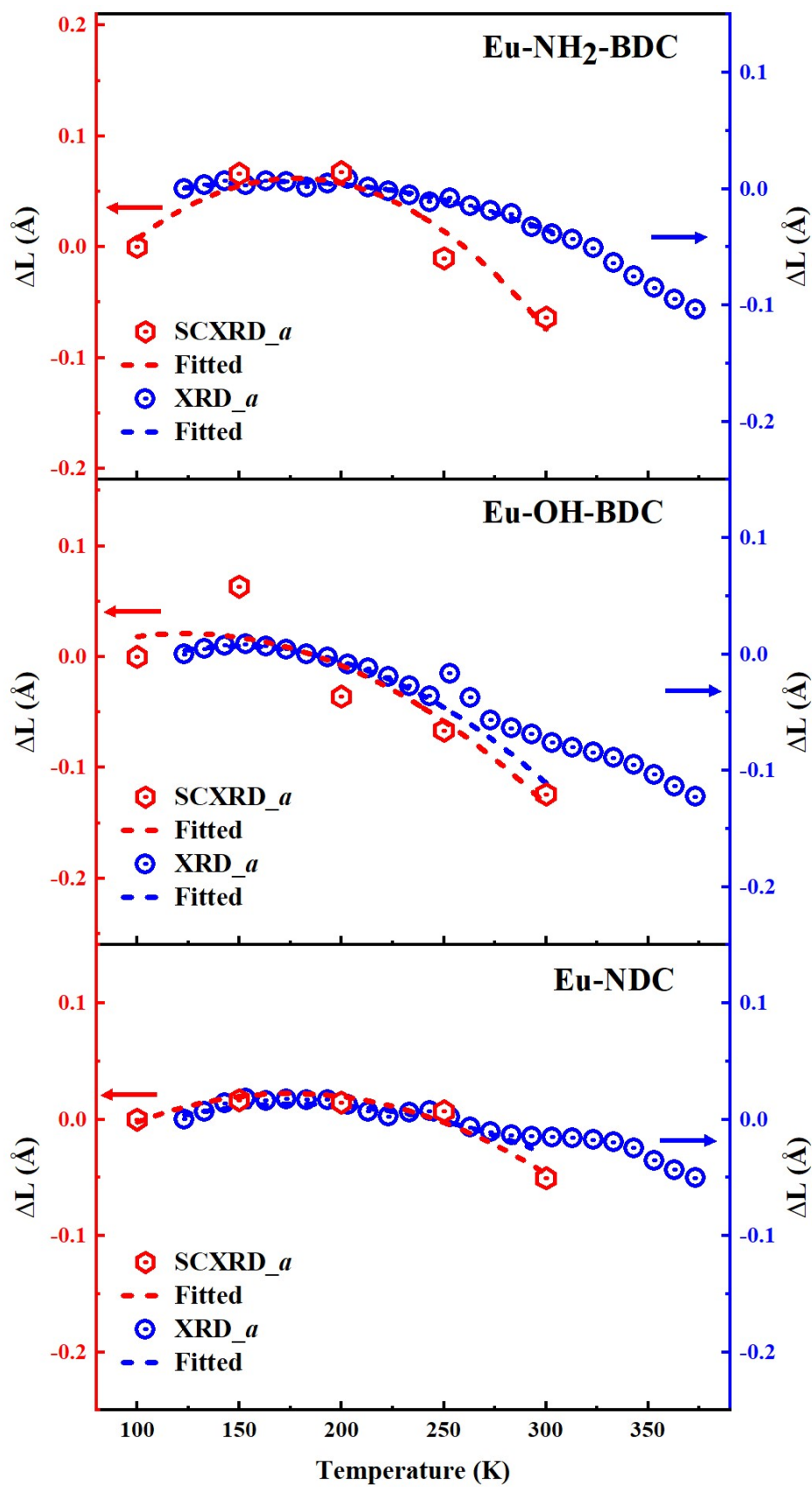


Figure S18. Comparison of SCXRD and XRD trends for (a) Eu-NH₂-BDC, (b) Eu-OH-BDC, and (c) Eu-NDC.

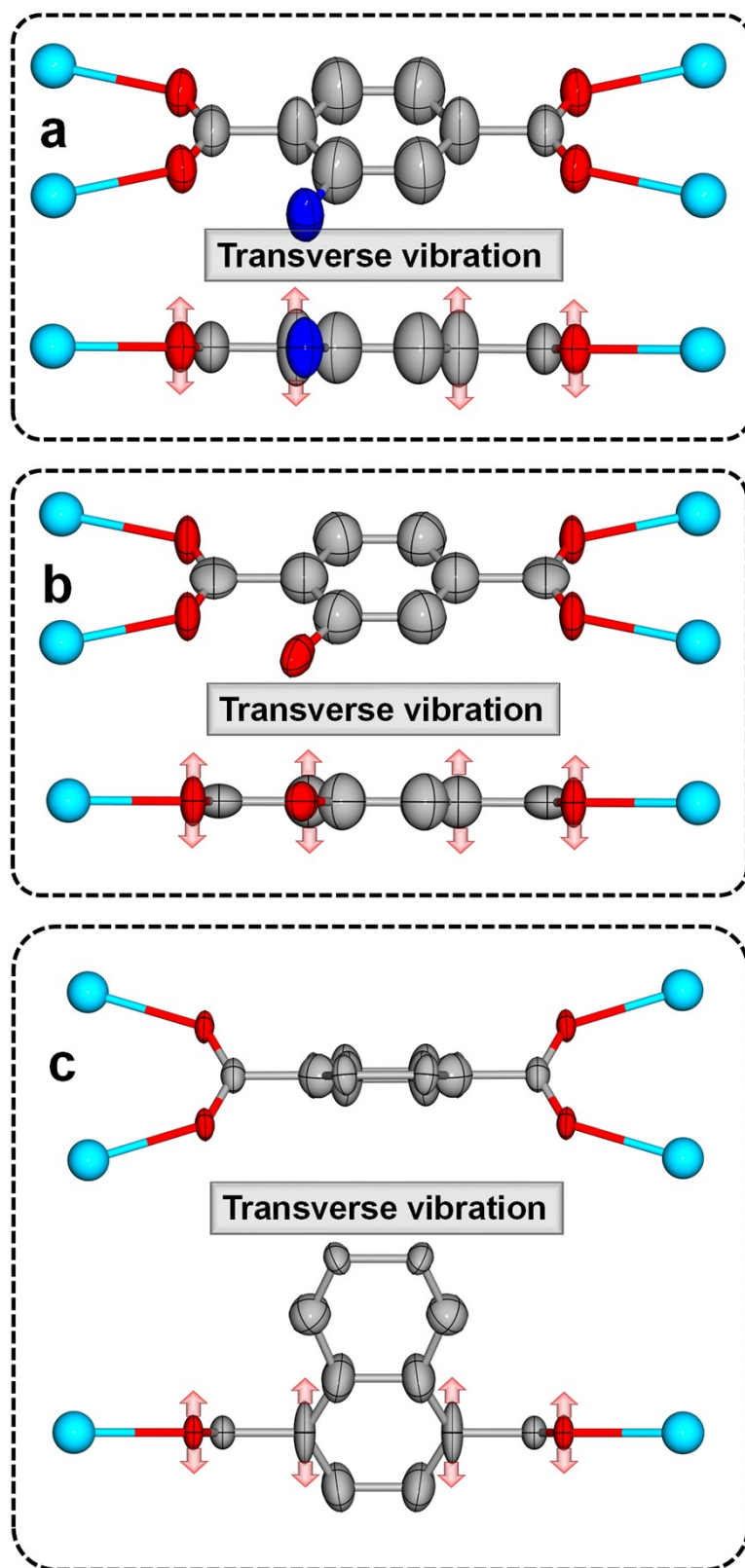


Figure S19. Atomic thermal vibrations in the crystal structures of (a) Eu-NH₂-BDC, (b) Eu-OH-BDC, and (c) Eu-NDC at 100 K. The size of ellipsoids is indicating the magnitude of ADPs.

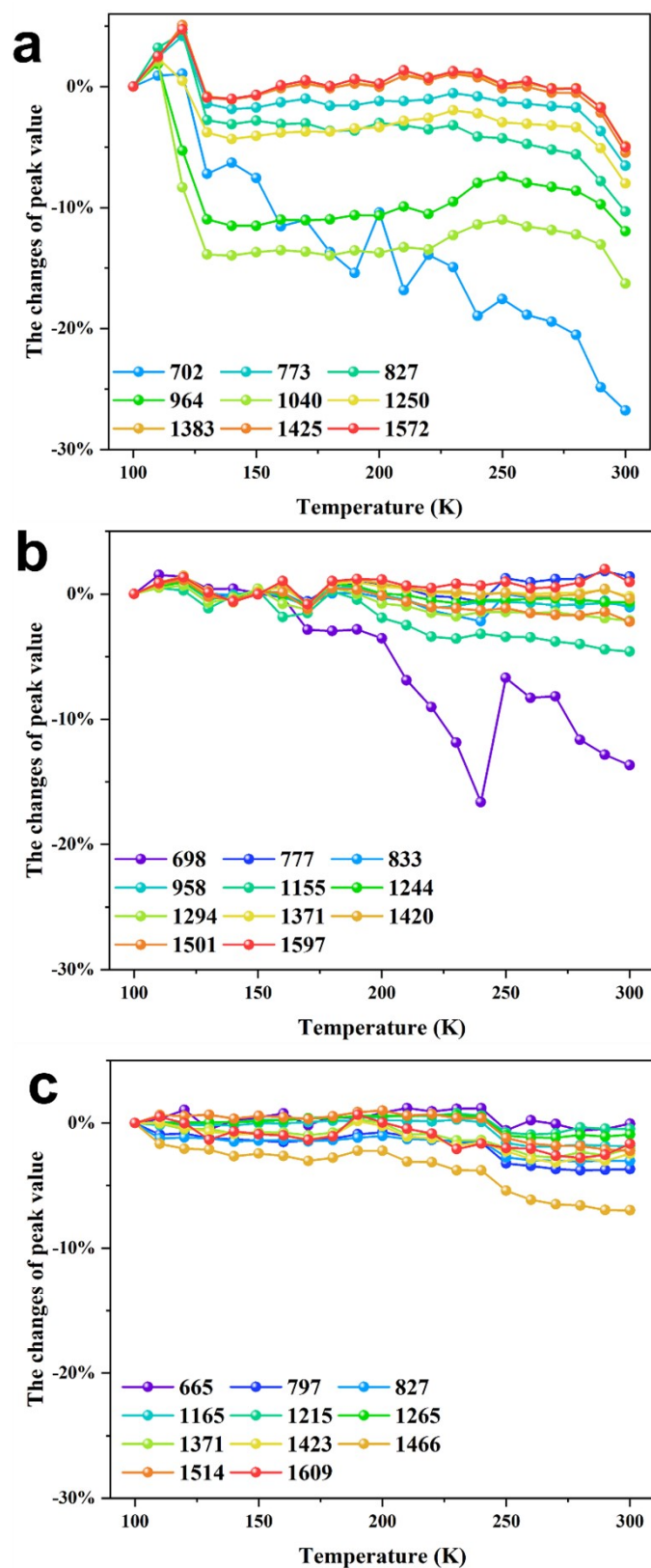


Figure S20. Change of Infrared peaks with temperature in (a) Eu-NH₂-BDC, (b) Eu-OH-BDC, and (c) Eu-NDC.

References

1. Macrae, C. F. *et al.* Mercury CSD 2.0 - new features for the visualization and investigation of crystal structures. *J. Appl. Crystallogr.* **41**, 466-470 (2008).
2. Sheldrick, G. M. A short history of SHELX. *Acta Cryst.* **A64**, 112-122 (2008).
3. Sheldrick, G. M. Crystal structure refinement with SHELXL. *Acta Cryst.* **C71**, 3-8 (2015).
4. Dolomanov, O. V. *et al.* OLEX2: a complete structure solution, refinement and analysis program. *J. Appl. Crystallogr.* **42**, 339-341 (2009).